Journal of Applied Fluid Mechanics, Vol. 3, No. 1, pp. 75-81, 2010.
Available online at www.jafmonline.net, ISSN 1735-3572, EISSN 1735-3645.
DOI: 10.36884/jafm.3.01.11881

CFD Numerical Simulation and Experimental Study of Effects of Screw-Sleeve Fitting Clearance upon Triangular Thread Labyrinth Screw Pump (LSP) Performance

R. Ma and K. Wang

Department of Mechanical and Electrical Engineering, Beijing University of Chemical Technology
Beijing 100029, China

Email: marm@mail.buct.edu.cn

(Received October 20, 2008; accepted April 11, 2009)

ABSTRACT

How the fitting clearance between the screw and the sleeve of a labyrinth screw pump (LSP) affects the pump performance and what law it follows are still unsolved problems for LSP design. So the fluid quasi-steady flow in the pump with different clearances is approximately modeled by the shear-stress transport k-ω model (SST k-ω model) in multiple reference frame (MRF) of CFD. The pump characteristics experiments are also carried out. In analyzing the simulated results, the fluid velocity in the pump is simplified as a linear superposition of a Couette flow dragged by the rotor screw and a pressure flow driven by the differential pressure of LSP. The CFD simulated results reveal that the clearance has scarcely effect on the drag flow. The mean axial pressure flow velocity in the clearance is the maximum and it increases with an increase of clearance. The leakage mainly occurs between the lands of screw and sleeve, and its rate can be simply estimated by leakage formulation for a narrow slot. With an increase in clearance, the pump maximum capacity changes little but the head and efficiency obviously decrease at the same flow rate. The changing tendency of simulated performances of the pump is in good agreement with the experimental results. At last, a set of modified relations between the pump performances and the relative diametrical clearance has been given, which can be applied to conveniently convert the LSP performance when the clearance changes.

Keywords: Labyrinth screw pump, Drag flow, Pressure flow, Fitting clearance, Leakage.

NOMENCLATURE

b thread lead(mm)
b_n normal width of thread land(mm)
c screw-sleeve fitting clearance(mm)
D nominal diameter of screw(mm)
g gravity acceleration
h depth of thread groove(mm)
H pump head,
K_f cell head coefficient
$K_{f,0.1}$ cell head coefficient of a pump with the relative diametrical clearance of 0.1
L axial length of the screw of LSP(mm)
Lc axial length of the modeled screw(mm)
m number of cells in axial direction
N_i hydraulic power of LSP
$N_{i,c}$ simulated hydraulic power for the modeled screw
Q flow rate
Q_f leakage through one region of the intersecting thread ridges
Q_{cl} total leakage through clearance
R radial coordinate in flow passage of the pump
s_D diametrical clearance between screw and sleeve, $2c$
s^* ratio of the diametrical clearance to the depth of thread groove $s^*= s_D/h$
u flow velocity(m/s)
u_c drag flow velocity by rotor(m/s)
u_p pressure flow velocity(m/s)
Δp pump pressure($\times 10^5$Pa)
z number of threads

Greek symbols
α helix angle of thread
ζ flow rate coefficient for the pump clearance
η pump efficiency
η_h CFD simulated efficiency without consideration of the pump mechanical friction loss
ρ fluid density

1. INTRODUCTION

A labyrinth screw pump (LSP) is also named a labyrinth screw seal (LSS). The LSS, as a seal device at shaft end with high rotational speed, must be accompanied with a shutdown seal for sealing leakage through the thread grooves of the screw and the sleeve during period of the machine shutdown (Golubiev, 1965). The LSP, as a pump to deliver chemical liquids such as weak acid and weak alkali, has being developed for decades (Golubiev, 1981). Especially in recent years, LSP has been gradually attracting attention from more and more pump manufacturers for having advantages of a simple structure, stable operation, long maintenance period and relatively high efficiency, up to 20%~30% in a range of pumps with specific speed lower than 10 (Ma *et al*. 2007, 2008).

In experimentally investigating LSP performances, we found that the screw-sleeve fitting clearance has a big influence on LSP performances. The pump lift decreases fast with an increase in clearance. Golubiev (1981) had experimentally found that with an crease in relative diametric clearance, the characteristics of LSP with triangular threads dropped most fast in comparison with other LSPs having rectangular, semicircular or trapezoidal threads. Han (1989) obtained a lift-capacity curve of the rectangular thread LSP with different clearances by numerical solving N-S equations. However, why LSP performances mainly involving the head and efficiency are so sensitive to the clearance and what relations between LSP performances and the clearance exist are problems necessarily solved in LSP design and its application. Sometimes, too small a clearance makes the pump head higher than an engineering technological requirement, which brings not only energy consumption but also heat generation in the rotor bearing system. Consequently, trimming clearance is often used as an approach to adjust the pump working conditions. However, how much to trim it completely depends on a designer's experience. There are also no relevant papers to this work**.** So based on CFD numerical simulation and the pump performance experiment, we have investigated the effects of the clearance between screw and sleeve on LSP performance.

2. CFD NUMERICAL SIMULATIONS

2.1 Geometric dimensions of the model

A triangular thread LSP can provide a higher head than those LSPs with rectangular, semicircular or trapezoidal shaped threads at the same diameter and working length of the rotor (Golubiev, 1981). At present, the commercial LSPs are all triangular thread LSPs. So we choose a triangular thread LSP to be modeled by CFD. The model's geometric dimensions on the normal cross-section is shown in Fig. 1, where both the screw with right-handed 27-threads and the sleeve with left-handed 27-threads have an effective axial fitting length of 150*mm* and a thread lead of 80*mm*. Considering the circumferential and axial periodicity of the simulated fluid field(Golubiev, 1965; Ma *et al.* 2008), the computational domain, formed by cutting the fluid channel with two helical radial sections separately located at the right and left side of one thread groove of the rotor, involves only one thread groove of the rotor and a sequence of corresponding stator grooves in multiple reference frame (MRF) of CFD. The circumferential angle of the fluid domain on cross-section perpendicular to z-axis is 13.34 deg., of which the intersecting thread ridge is 1.43 deg. (Fig. 2). The axial length of the computational model is 40mm and the screw-sleeve fitting clearance is 0.2, 0.28, 0.32 and 0.4mm, respectively.

2.2 CFD grid generation and solution

Because of irregularity of the fluid boundaries, unstructured tetrahedral grids are used to mesh the grooves of the screw and the sleeve and more than five layers of prism grids with edge no longer than 0.3mm are used to mesh the clearance between the screw and the sleeve. The mesh number so obtained is about 9×10^5, of which the simulated result is independent. The area-weighted wall y+ for the walls of the screw and the sleeve is less than 30-40, and for the wall of the clearance is about 10 (Tide and Babu, 2009; Paul *et al.* 2008). This is reasonable when the option of transition flows in k-w SST model is not active.

Inlet and outlet of the modeled region are set as pressure-inlet and pressure-outlet separately (El-Sadi and Esmail, 2006; Kumar *et al.* 2009), the screw and sleeve walls as the wall boundaries and the interfaces between the fluid zones as the interior. The other faces are all rotary periodic boundaries with respect to the pump z-axis (Fig. 2).

The screw rotates in left direction at rotating speed of 2900 revolutions per minute, and the fluid in the grooves of screw and sleeve will be pumped along the positive axial direction. The working fluid is incompressible water with a normal temperature and constant properties. Continuity and momentum equations are discretized by the second-order upwind schedule and solved by the uncoupling implicit SIMPLE algorithm. Since the fluid flow in LSP is a turbulent flow with low Reynolds number (Ma *et al.* 2008), the k-ω SST (shear stress transport) model was used (Tide and Babu, 2009; Viti *et al.* 2007; Paul *et al.* 2008; Yan, 2006), in which the model constants have default values. The detailed information about the model validation and the treatment of the computational data on the flow rate and the differential pressure were given by Ma *et al.* (2008).

The total axial moment imposed on the rotating screw of LSP is also simulated by CFD. Then the hydraulic power of the screw is the product of the total moment with the angular velocity of the screw. The CFD simulated result shows that the tangential resultant pressure on the screw walls distributes uniformly along z-axis. For this condition, the hydraulic power of the pump is approximately calculated by Eq. (1)

$$N_i = \mathrm{L}\cdot N_{i,c} / L_c \tag{1}$$

Assuming the mechanical friction power of the pump as 1, then the simulated efficiency η_h (Eq. 2) is used to account for the pump efficiency.

$$\eta_h = \rho g Q H / N_i \tag{2}$$

3. RESULTS ANALYSIS

3.1 Theory for Analysis

Considering the ratio of the thread groove depth to the rotor diameter being small, Bilgen and Akgungor (1973) simplified the fluid flow in LSP as a linear superposition of a Couette flow dragged by the rotor screw and a pressure flow driven by the differential pressure of LSP between two infinite parallel plates with thread grooves. That means the flow velocity u in thread grooves is the vector sum of the drag flow velocity u_c and the pressure flow velocity u_p. u is expressed by Eq. (3)

$$u = u_c + u_p \tag{3}$$

Consequently, the pump flow rate is the algebraic sum of the Couette flow rate and the pressure flow rate. Based on Bilgen's theory, the CFD simulated flow field is decomposed as a drag flow and a pressure flow. The pressure flow velocity is approximately obtained by Eq. (3) if both the Couette flow field at Δp=0*MPa* and the total flow field at $\Delta p \neq 0$ *MPa* are simulated by CFD.

3.2 Mean Axial Couette flow

Figure 3 is the area-weighted average axial Couette flow velocity at the different cylindrical sections in LSP with clearances of 0.2, 0.28, 0.32 and 0.4mm, respectively. The computational differential pressure between two ends of the rotor is zero. It is seen that the drag flow velocity distribution along the radial direction is a similar parabola distribution, and the maximum velocity is approximately at *R=49mm*. The velocity distributes uniformly over a range of *R=47~49mm*, and at the bottom of the rotor groove, it decreases to the minimum. The mean axial velocity drops fast in sleeve groove and reaches zero near the bottom of sleeve groove. In general, Fig. 7 shows that LSPs with different clearances have nearly the same Couette flow velocity distributions, and the clearance has scarcely effect on the Couette flow.

3.3 Mean Axial Pressure Flow

The area-weighted average axial pressure flow velocity at the corresponding cylindrical sections is shown in Fig. 4. The computational differential pressure is 0.2, 0.4 and 0.6*MPa*, respectively, and the simulated model has the clearance of 0.2*mm*. The pressure flow flows from the high-pressure end to the low-pressure end in LSP. Its direction is opposite to that of the Couette flow. Figure 4 indicates that, due to the thread action, the pressure flow velocity distribution between the screw and the sleeve is not a similar parabola distribution as that of the pressure flow between two parallel smooth plates. It is the maximum in the clearance and is higher in the screw grooves than in the sleeve grooves.

Additionally it decreases when approaching the bottom of the sleeve grooves while increases when approaching the bottom of the rotor grooves, where it even reaches a maximum velocity with an increase in the computational differential pressure. The reasons for such velocity distribution could be that the fitting clearance is the shortest passage connecting the high-pressure region to the low-pressure region of the pump and has the smallest flow resistance. However, the liquid in thread grooves is not only retarded by the threads of screw and sleeve but also acted on an axial strong driven force by the rotating screw threads. So the pressure flow velocity is the maximum in the clearance and is bigger in stator groove than in rotor groove. Near the bottom of the rotor groove, the axial driven force of the rotor thread on fluid gradually becomes weak so that a maximal pressure flow velocity also appears there.

Figure 5 is the radial distribution of the mean axial pressure flow velocity at the computational pressure of 0.2MPa for the computational model with clearances separately being 0.2, 0.28, 0.32 and 0.4*mm*. It obviously shows that the bigger the clearance, the bigger the velocity in the clearance. The velocity in stator groove increases slightly and in rotor groove it has almost no change. The differential pressure is well known a fundamental cause to fluid leakage, so we concluded that owing to the more clearance leakage, the capacity of the pump with a bigger clearance will decrease under the same differential pressure.

3.4 Mean Axial Velocity in Fitting Clearance

Figures 6 and 7 are separately the circumferential distributions of the average axial velocity and the static pressure on axial section z=26.68mm of the computational model with the clearance of 0.2mm. The computational differential pressure is 0.4*MPa*. Figure 6 displays the mean axial velocity between the lands of screw and sleeve is the biggest in the leakage direction. In the clearance, it increases with an increase in radius and decreases when approaching the inner surface of the sleeve. In a cell momentarily formed by two screw threads and two sleeve threads, the liquid in rotor groove flows from the rotor pressure side toward the suction side of stator groove and brings momentum with pumping direction into the liquid in stator groove while the liquid in stator groove flows from the stator pressure side back to the suction side of rotor groove and brings momentum with the leakage direction into the liquid of rotor grooves (Ma *et al.* 2008). So the direction of the fluid flow in the clearance changes circumferentially from the pumping direction near the pressure side of the screw groove in a cell to the leakage direction near the suction side of it.

In Fig. 7, the static pressure at the cell center decreases because of a strong vertex formed in the stator groove. Comparing Fig. 6 and Fig. 7, the fluid flow in the intersecting thread ridges has characteristics of the biggest axial velocity and the smallest static pressure and can be regarded as a typical throttled leakage flow.

3. 5 Leakage through Fitting Clearance

The leakage rate through the intersecting thread ridges can be determined by a leakage formula of a slot with a clearance of $s_D/2$ (Eser and Kazakia, 1995; Eser, 2002; Yucel, 2004). The differential pressure between the two axial adjacent cells is supposed as $\frac{\Delta p}{m} = \frac{\Delta p b}{zL}$, and then the leakage through one overlapped region is expressed as

$$Q_f = \zeta \frac{b_n}{\sin\alpha} \frac{s_D}{2} \sqrt{\frac{2\Delta p b}{zL\rho}} \tag{4}$$

where b_n is the normal width of a thread land (Fig. 2). ζ is the leakage coefficient accounting for the effects of the clearance geometry, its dimensions and leakage fluid type on leakage rate.

One thread has *z* overlapped regions in a circumference (Golubiev, 2005), thus the total leakage through clearance is given by

$$Q_{cl} = \zeta \frac{b_n s_D}{2\sin\alpha} \sqrt{\frac{2z\Delta p b}{L\rho}} \tag{5}$$

Considering a correction to the leakage length, which clearly exceeds the circumferential length of the overlapped region, let the leakage coefficient ζ be 0.81, which approaches the coefficient 0.716 of the air leakage through labyrinth seal (Eser and Kazakia, 1995; Yucel, 2004). The comparison between the calculated leakage by Eq. (5) and the simulated result is shown in Fig. 8 with the pump head as an ordinate. It shows they are in better agreement. The deviation between them might be brought about by assuming the flow coefficient ζ as a constant. In fact, the coefficient ζ is a function of the relative clearance s_D/h, and it becomes small with a decrease in s_D/h.

3.6 Clearance Impacts on LSP Pumping Performance

Under the same differential pressure and the nearly unchanged Couette flow capacity, the bigger the clearance, the more the leakage, so the pump total flow capacity decreases. Figure 9 is the simulated lift-capacity curve of the triangular thread LSP with the clearances of 0.2, 0.32 and 0.4mm, respectively. Obviously, H-Q curve becomes more and more flat with an increase in clearance and the pump head and efficiency fall under the same flow rate.

The clearance affects the pump head from the following two aspects. Firstly, the leakage rates through the bigger clearance increase and lead to decrease in pump head. Secondly, Ma *et al.* (2008) proposed that when the liquid in rotor grooves flows through the bigger clearance into the stator grooves, it will lose more momentum and energy into the liquid in bigger clearance than in smaller clearance. As a result, the momentum transfer between the liquid in a cell becomes weak and the total effective energy of the liquid decreases as well as the pump total head. So the pump head decreases more quickly with an increase in clearance.

Figure 10 shows the variation of the relative cell head coefficient $K_f/K_{f,0.1}$ of the triangular thread LSP with the relative diametrical clearance s_D/h, where the data is obtained by CFD simulation and Golubiev's (1981) experimental results. Based on the pumping mechanism of LSP and the theoretical analysis, Ma and Wang obtained an empirical Eq. (6) relating the relative cell head coefficient and the relative diametrical clearance for the triangular thread LSP.

$$K_f / K_{f,0.1} = 1.785/(1+s^*)^6 \tag{6}$$

Substituting Eq. (6) into the conversion relations betwe en LSP performances and the relative diametrical cleara nce proposed by Ma *et al.* (2007), a set of modified rela tions with a tidier and simpler form are derived.

$$\begin{aligned} \frac{Q'}{Q} &= \frac{h'(1-s^{*'}/2)}{h(1-s^*/2)} \\ \frac{H'}{H} &= \frac{(1+s^*)^6}{(1+s^{*'})^6} \\ \frac{\eta'}{\eta} &= \frac{1-s^{*'}}{1-s^*} \end{aligned} \tag{7}$$

Based on Eq. (7), the pump performance curves, *H-Q* and η-*Q*, are converted from the clearance of 0.2 to 0.32 and 0.4*mm*. The transformed curves are plotted by the dashes in Fig. 9, where the pump maximum capacity is unnecessarily converted for it's nearly independence of the clearance. In Fig. 9, the converted result is clearly in good agreement with the CFD simulation. However, the converted head gradually becomes lower than the simulated one when the flow rate increases.

From Eq. (7), we also obtain the conversion equation for the pump power.

$$\frac{N'}{N} = \frac{Q'H'\eta}{QH\eta'} \tag{8}$$

4. Experimental Study and Result Analysis

Details on establishment of the experimental equipment and selection of the experimental instruments for LSP performance are presented by Ma *et al.* (2007). Two LSPs used for experiments have rotor diameter of 100mm and 110*mm*, respectively, thread lead 88*mm*, fitting clearance 0.1*mm* and thread groove depth 3.2*mm*. After being trimmed, the clearance and the thread groove depth become 0.16*mm* and 3.17*mm* separately.

The characteristic curves for the two pumps are separately plotted in Fig. 11 and Fig. 12, in which the transformed curves of *H-Q* and η-*Q* from the clearance

of 0.1 to 0.16*mm* were plotted by the dashes based on the modified equation (7). It shows that the experimental trends of the pump flow rate, head and efficiency are in good agreement with the CFD numerical simulation, and the converted head by Eq. (7) is nearer to the experimental head than the converted equation provided by Ma *et al.* (2007). It is also seen that the converted efficiency is higher a little than the experimental one and the reason could be that the hydraulic losses brought by increasing clearance is neglected in the conversion efficiency.

5. CONCLUSION

By the CFD numerical simulation and the pump characteristics experimental study of the triangular thread LSP with different clearances, some conclusions are drawn as follow.

1. The fitting clearance between the screw and the sleeve has little effect on the drag flow of the rotor and it could be considered to have no effect on it.
2. The mean axial pressure flow velocity is the maximum in the clearance and the maximum increases with the clearance at the same differential pressure.
3. The clearance leakage mainly takes place in the intersecting thread ridges. It can be estimated by the leakage equation for a slot, and the estimation is in better agreement with the CFD simulated result.
4. The clearance increasing will lead to the momentum transfer between the liquid in a cell becoming weak and the total effective energy decreasing as well as the pump head and efficiency. The changing tendency of the triangular thread LSP performances simulated by CFD coincides with the pump experimental result.
5. Equation (7) to predict the change of flow rate, lift and efficiency of the triangular thread LSP with the relative diametrical clearance can provide the better predicted result. It is simple and convenient for application of Eq. (7) to the pump working condition adjustment in engineering.

REFERENCES

Golubiev, A.I. (1965). Studies on seal for rotating shafts of high-pressure pumps. *Wear* 8, 270-288.

Golubiev, A.I. (1981). *Labyrinth-Screw Pumps and Seals for Corrosive Media*. 2nd revised and extended edition (in Russia), Mashinostroenie, Moscow.

Bilgen, B. and A.C. Akgungor (1973). The turbulent double screw pump-theory and experiment. *Proceedings of the 6th International Conference on Fluid Sealing*, February 27th-March 2nd, Munich, German Federal Republic G4, 45-60.

Han, G.J. (1989). *Study of Labyrinth Screw Pump and Its Combined Seal*. PhD Thesis, Beijing University of Chemical Technology, Beijing, China (in Chinese).

Ma, R.M., K.S. Wang and J.Z. Li (2008). Study on Pumping Mechanism of Labyrinth Screw Pump by CFD Numerical Simulation and Pump Performance Experiments. *Lubrication Engineering* 2, 75-79 (in Chinese).

Ma, R.M., K.S. Wang and J.Z. Li (2007). Experimental study of labyrinth screw pump characteristics. *Fluid Machinery* 12, 1-4 (in Chinese).

Tide, P.S. and V. Babu (2009). Numerical predictions of noise due to subsonic jets from nozzles with and without chevrons. *Applied Acoustics* 70, 321-332.

Viti, V., G. Huang and P. Bradshaw (2007). Numerical study of stress-transport turbulence models: Implementation and validation issues, *Computers & Fluids* 36, 1373-1383.

Paul, S.S., S.J. Ormiston and M.F. Tachie (2008). Experimental and numerical investigation of turbulent cross-flow in a staggered tube bundle. *International Journal of Heat and Fluid Flow* 29, 387-414.

Yan, C. (2006). *Computational Methods and Applications for Fluid Dynamics*. Press of Bejing University of Aeronautics and Astronautics (in Chinese), Beijing, China.

Zhang, J.Z. and Y.P. Li (1987). Experimental Study of Labyrinth Screw Seal. *Seal and Anticorrosion* 4, 41-49 (in Chinese).

El-Sadi, H. and N. Esmail (2006). Simulation of three-dimensional transient performance in micro-pump. *Sensors and Actuators* B 115, 510-518.

Kumar, S., J.M. Bergada and J. Watton (2009). Axial piston pump grooved slipper analysis by CFD simulation of three-dimensional NVS equation in cylindrical coordinates. *Computers & Fluids* 38, 648-663.

Eser, D. and J.Y. Kazakia (1995). Air flow in cavities of labyrinth seals. *International Journal of Engineering Science* 33, 2309-2326.

Eser, D. (2002). Rotordynamic coefficients in stepped labyrinth seals. *Computer Methods in Applied Mechanics and Engineering* 199, 3127-3135.

Golubiev, A.I. and E.I. Pyatigorskaya (2005). Efficiency coefficients of a labyrinth pump. *Chemical and Petroleum Engineering* 41(5), 21-23.

Yucel, U. (2004). Calculation of leakage and dynamic coefficients of stepped labyrinth gas seals. *Applied Mathematics and Computation* 152, 521-533.

Ma, R.M. and K.S. Wang. (2009) Modeling of Pumping Performance of Labyrinth Screw Pump (LSP) by 2D Reynolds Stress Equations. *Journal of Fluids Engineering* (accept).

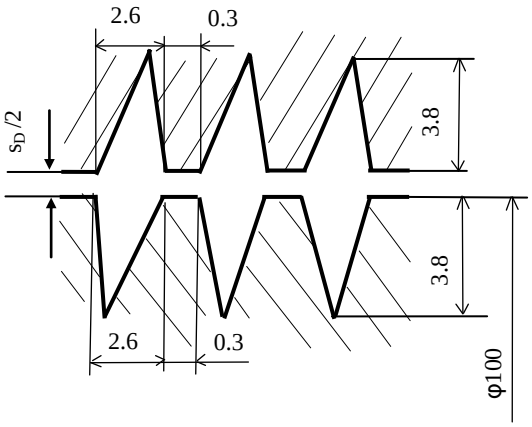

Fig.1. Geometric dimensions of the modeled triangular thread for LSP

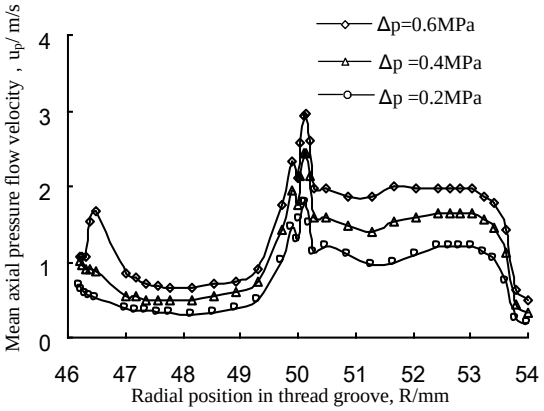

Fig. 4. Radial distributions of the mean axial pressure flow velocity at computational differential pressures of 0.2, 0.4 and 0.6MPa, respectively.

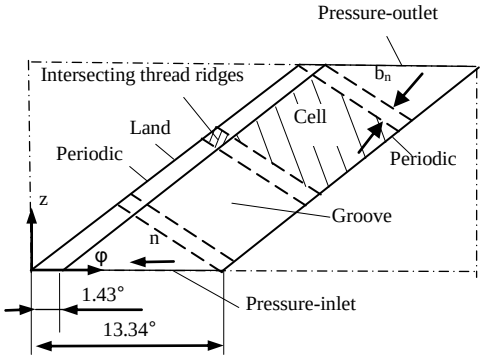

Fig. 2. A schematic plan of the simulated model —— Rotor – – – Stator

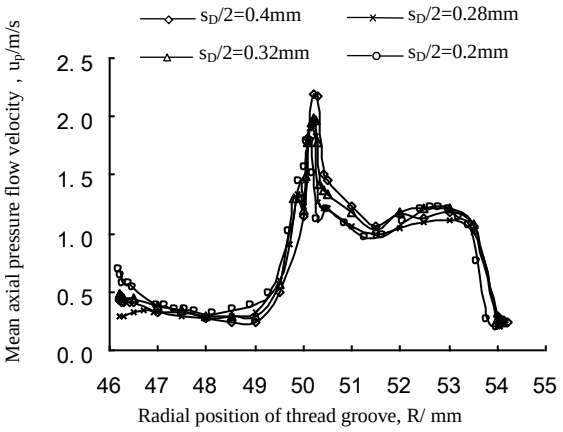

Fig. 5. Radial distributions of the mean axial pressure flow velocity at computational differential pressure of 0.2MPa for LSPs with different clearances.

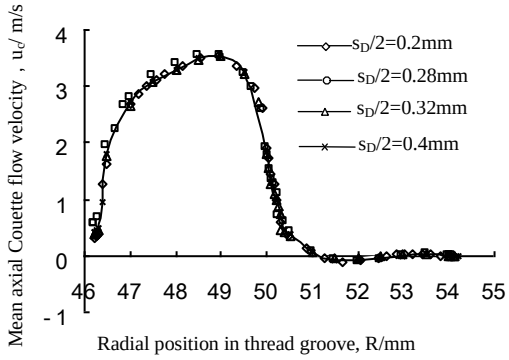

Fig. 3. Radial distribution of the mean axial Couette flow velocity in LSP with different clearances

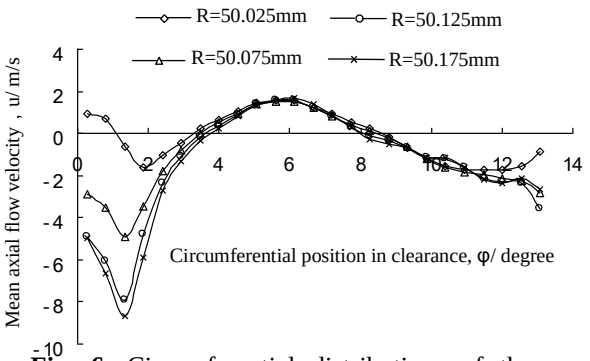

Fig. 6. Circumferential distributions of the mean axial flow velocity at different radius in clearance.

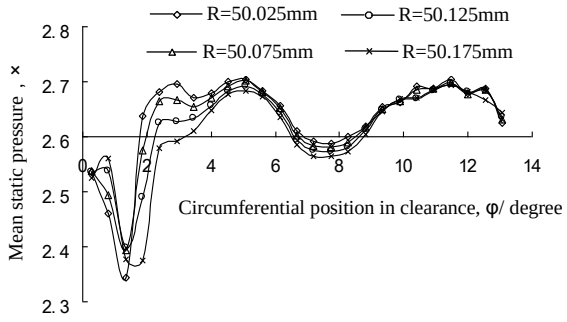

Fig. 7. Circumferential distributions of the mean static pressure at different radius in clearance

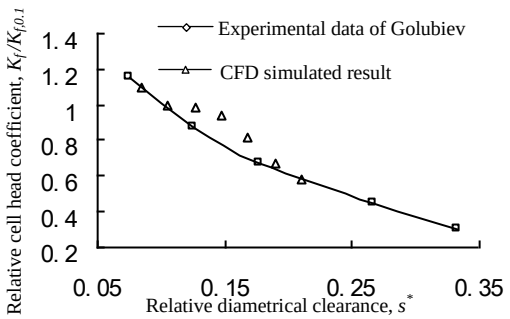

Fig. 10. The relative cell head coefficient versus the relative diametrical clearance for triangular thread LSP

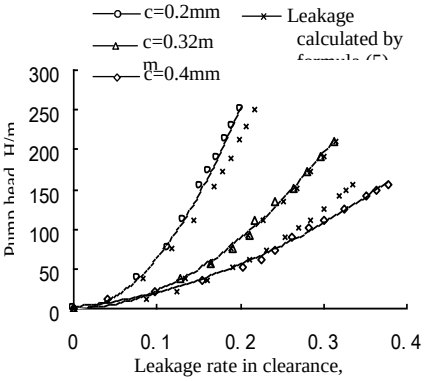

Fig. 8. Comparison between the simulated leakage and the estimated result by equation (5)

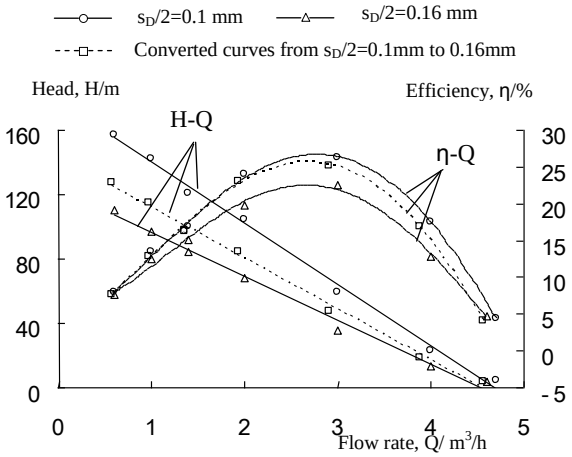

Fig. 11. Experimental performance curves for LSP with type of Φ100×88×27 and different radial clearances of 0.1 and 0.16mm, where *D* is 100mm, *b* is 88mm and *z* is27.

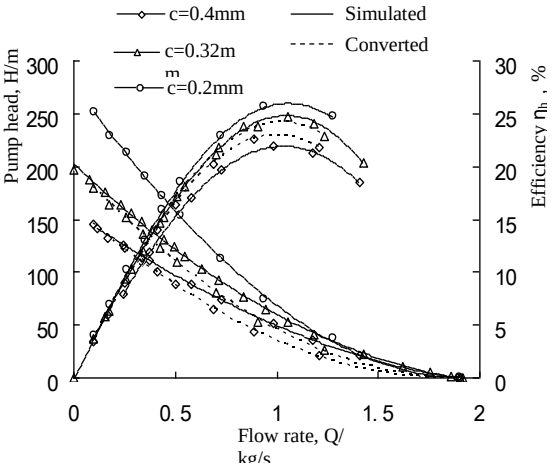

Fig. 9. CFD simulated performance curves of the triangular thread LSPs with different clearances.

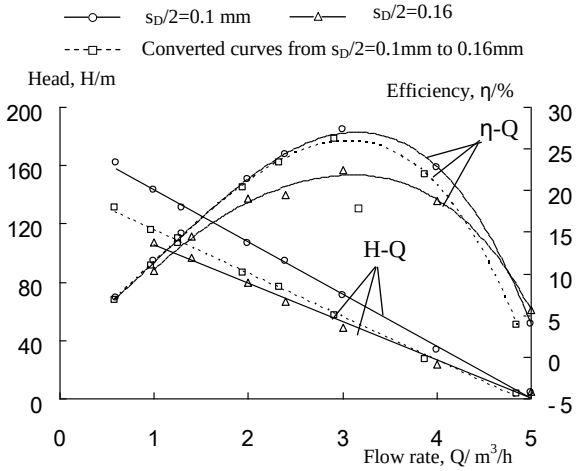

Fig. 12. Experimental performance curves for LSP with type of Φ110×88×27 and different radial clearances of 0.1 and 0.16mm, where *D* is 110mm, *b* is 88mm and *z* is27.